

## THE EFFECTS OF FOAMING AGENT AND SURFACTANT ON ALKALI ACTIVATED MATERIALS AS AN ADSORBENT FOR LEAD IONS ADSORPTION

Lead, a hazardous environmental metal, has been widely used in various applications, either pure or alloyed with other metals. This study investigates the impact of foaming agents and surfactants content on the physical properties of metakaolin-based alkali activated materials. Additionally, it seeks to assess the effectiveness of metakaolin-based AAM adsorbent in removing lead ions. The research uses varying percentages of foaming agents (1 wt.%, 1.25 wt.%, and 1.5 wt.%) and surfactants (1 wt.%, 3 wt.%, and 5 wt.%). Water absorption, density and porosity tests were used to evaluate the metakaolin-based alkali activated adsorbent's physical properties. Scanning Electron Microscopy (SEM) was used to study the morphology of the adsorbent. In addition, the adsorption test was investigated to determine the lead ion removal in the AAM adsorbent. The ion removal performance of metakaolin based alkali activated materials was evaluated based on different amounts of foaming agent and surfactant. A lead (II) solution was prepared in distilled water and used in the adsorption test. An adsorption test was carried out to determine the effectiveness of AAM with a foaming agent and surfactant, which showed that it could be suited to many harsh conditions. This study successfully identified the optimal parameters for achieving maximum efficiency in lead ion removal, featuring a concentration of 1.25 wt.% of foaming agent and 3 wt.% of surfactants. These findings hold significant promise for the advancement of effective adsorbents, particularly in the realm of wastewater treatment processes.

*Keywords:* Alkali activated material; wastewater treatment; foaming agent; heavy metal removal

### 1. Introduction

The global concern over environmental pollution caused by various types of waste has grown significantly. These pollutants' accumulation seriously threatens human health, wildlife, and the ecosystem. Consequently, extensive efforts have been undertaken to address this issue by exploring methods to reduce pollution and develop sustainable wastewater treatment techniques. Wastewater treatment, also known as sewage treatment, involves the removal of impurities from wastewater before it is discharged into natural water bodies such as rivers, lakes, estuaries, and oceans [1,2].

Dealing wastewater containing heavy metals into the environment has become a growing problem, directly or indirectly, due to rapid industrial expansion in sectors such as battery manufacturing, mining, metal plating, pesticide production, and fertilizer usage [3,4]. Heavy metals possess an inorganic structure that prevents them from decomposing naturally, leading to their accumulation as hazardous and carcinogenic substances in living

organisms. Common examples of such heavy metals include mercury, lead, copper, zinc, nickel, chromium, and cadmium, frequently encountered in industrial wastewater [5,6].

Among these heavy metals, lead has been identified as a particularly hazardous element with significant detrimental effects on human health. Therefore, the Environmental Protection Agency (EPA) has set the maximum contamination level of lead in water at zero [7,8]. Even small amounts of lead can profoundly impact human health, especially in infants, children, and fetuses, compared to adults. Geopolymers or alkali activated materials have emerged as a potential solution for waste recycling; however, the presence of hazardous materials like lead in certain waste materials, for example, crushed cathode ray tube (CRT) glass, necessitates specialized chemical and electrochemical processes for their recovery [9,10].

Alkali-activated materials (AAM) and their subgroup, geopolymers, are widely recognized as low-CO<sub>2</sub> binders and play a crucial role in promoting the circular economy by converting inorganic wastes into valuable products [11,12]. While

<sup>1</sup> UNIVERSITI MALAYSIA PERLIS (UNIMAP), FACULTY OF MECHANICAL ENGINEERING & TECHNOLOGY, 02600, ARAU, PERLIS, MALAYSIA

<sup>2</sup> UNIVERSITI MALAYSIA PERLIS (UNIMAP), CENTER OF EXCELLENCE GEOPOLYMER AND GREEN TECHNOLOGY (CEGEOGTECH), 01000, PERLIS, MALAYSIA

<sup>3</sup> UNIVERSITI MALAYSIA PERLIS (UNIMAP), FACULTY OF CHEMICAL ENGINEERING & TECHNOLOGY, 02600, ARAU, PERLIS, MALAYSIA

\* Corresponding author: [wannastura@unimap.edu.my](mailto:wannastura@unimap.edu.my)



AAM have been primarily utilized in various applications, their potential in water and wastewater treatment is a relatively new area of exploration [13,14]. AAM, characterized by their amorphous aluminosilicate nature, are versatile and find applications as adsorbents, membranes, filtration media, photocatalysts, and solidification agents in water and wastewater treatment processes [3,15].

Furthermore, metakaolin (MK), a calcined form of kaolin clay, has gained significant interest in recent years due to its unique properties [16,17]. Metakaolin-based alkali activated materials have effectively removed heavy metals from wastewater through adsorption, offering a promising solution for industrial applications that benefit the environment and society [18,19]. Moreover, the sustainable production method of metakaolin, which involves utilizing waste streams or by-products and consuming minimal energy, positions it as an environmentally friendly alternative to other materials [20].

Adsorption has emerged as a widely recognized and cost-effective method for treating heavy metal-contaminated wastewater. It is a versatile process tailored to produce high-quality treated effluent in various scenarios [21,22]. Furthermore, adsorbents can be regenerated using appropriate desorption methods, as adsorption is often reversible [23]. The fundamental concept of adsorption involves the attachment of a solute, referred to as the adsorbate, to the surface of a porous solid known as the adsorbent [24,25]. This process facilitates the separation of the solute from the solution.

However, there is limited specific information and understanding regarding pore distribution and microstructure, especially when combining raw materials with high silica and alumina content with foaming agents during the fabrication process of porous alkali-activated materials for efficient adsorption of heavy metals in wastewater treatment. Using chemical foaming agents to generate porous structures with varying pore sizes in AAM poses challenges due to rapid chemical reactions and limited control over the process. The study focuses on alkali-activated materials (AAM), a relatively sustainable novel class of materials with potential applications in various industries, including construction and environmental remediation. Investigating the effects of optimal concentrations of foaming agents and surfactants on the adsorption capacities of AAM provides valuable insights into the potential use of these materials as highly efficient adsorbents in removing lead ions metal aligning with global efforts to minimize the environmental footprint of water treatment processes.

## 2. Experiment

### 2.1. Materials

The aluminosilicate materials used in this research are kaolin purchased from Kaolin (Malaysia) Sdn. Bhd., Bidor, Perak, Malaysia. First, it will be calcined to produce metakaolin at 850°C for 2 hours at a 5°C/min heating rate. This research

prepared a 10 M sodium hydroxide (NaOH) solution using a 99% pure NaOH pellet obtained from Brenntag Sdn. Bhd., located in Shah Alam, Selangor, Malaysia. The pellet was dissolved in 1000 ml of distilled water in a volumetric flask. The selection of a 10 M concentration of sodium hydroxide (NaOH) in metakaolin based AAM was based on the research conducted by Jaya et al. [26]. The researchers found that a 10 M NaOH solution demonstrated specific characteristics of higher porosity and lower density desirable for its application in metakaolin-based alkali-activated materials as an adsorbent material. The research's technical-grade sodium silicate,  $\text{Na}_2\text{SiO}_3$ , was provided by South Pacific Chemical Industries Sdn. Bhd. (SCPI) of Malaysia which had a composition of 30.1%  $\text{SiO}_2$ , 9.4%  $\text{Na}_2\text{O}$ , and 60.5%  $\text{H}_2\text{O}$  (with a  $\text{SiO}_2/\text{Na}_2\text{O}$  ratio of 3.20).  $\text{Na}_2\text{SiO}_3$  liquid is a transparent liquid easily dissolved in water.

A hydrogen peroxide solution was prepared as the foaming agent to enhance the porous structure of adsorbents. The 3 wt.% hydrogen peroxide was diluted from a 30 wt.%  $\text{H}_2\text{O}_2$  solution obtained from Sigma Aldrich in Malaysia. Additionally, a surfactant, Tween 80 or polysorbate 80, was included in the mixture. This surfactant, consisting of 70% oleic acid (with the remaining content primarily linoleic, palmitic, and stearic acids), was obtained from Sigma Aldrich in Malaysia. The surfactant was added to decrease the surface tension and drainage of the alkali-activated materials, serving its common function in such applications.

Synthetic wastewaters with lead (Pb) were generated by preparing a stock solution of  $\text{Pb}^{2+}$  ions. This stock solution was created by dissolving a high-quality analytical grade reagent, lead dinitrate salt ( $\text{Pb}(\text{NO}_3)_2$ ), obtained from Sigma Aldrich with a purity of 99.5% in distilled water.

### 2.2. Preparation of Metakaolin based Alkali Activated Materials as an Adsorbent

400 g of sodium hydroxide pellets and 1000 ml of distilled water were initially added to a volumetric flask to prepare the 10 M sodium hydroxide solution. It was then followed by the addition of sodium silicate to the mixture. An alkaline activator solution made of sodium hydroxide (NaOH) and sodium silicate ( $\text{Na}_2\text{SiO}_3$ ) was combined with metakaolin powder at a set 0.8 solid-to-liquid ratio by mass, which was chosen based on prior research. The mixture was mechanically stirred at room temperature for 5-7 minutes until all the substance had dissolved. The paste was then incorporated with hydrogen peroxide and Tween 80.  $\text{H}_2\text{O}_2$  dosages of 1 wt.%, 1.25 wt.% and 1.5 wt.% by mass of metakaolin were applied by fixing the solution with 1 wt.% Tween 80. The tween 80 dosage was then changed between 1 wt.%, 3 wt.%, and 5 wt.% by mass of metakaolin based on the optimal porosity and water absorption of the hydrogen peroxide content. A control sample without a foaming agent was also tested as a comparison. This control sample serves as a reference point to assess the specific effects and contributions of the foaming agent on the properties or characteristics being

investigated. The metakaolin based alkali activated materials foams were shaped into 1-2 cm sphere-shaped and cured at 60°C for 24 hours. After the curing process, the samples were kept at room temperature until the day of testing.

### 2.3. Test and analysis method

The porosity of metakaolin-based AAM was determined following ASTM C642 [27] and calculated using Eq. (1). The density of the metakaolin based electronic densitometer MD-3005 determined AAM according to ASTM D792 [28].

$$\begin{aligned} \text{Percent Porosity (\%)} &= \\ &= \frac{\text{Wet weight (g)} - \text{Dry weight (g)}}{\text{Dry weight (g)} - \text{Suspended weight (g)}} \times 100 \end{aligned} \quad (1)$$

Water absorption tests were performed according to ASTM D570 [29] by immersing specimens in distilled water at room temperature. Before being weighed on a digital scale, each sample was removed from the water and wiped to eliminate surface water. Eq. (2) was used to calculate the water absorption percentage.

$$\begin{aligned} \text{Water absorption (\%)} &= \\ &= \frac{\text{Wet weight (g)} - \text{Dry weight (g)}}{\text{Dry weight (g)}} \times 100 \end{aligned} \quad (2)$$

Characterization, physical testing, and mechanical testing were the three divisions of the testing procedure performed in this study. X-ray fluorescence (XRF) and scanning electron microscope (SEM) are used to analyze the chemical composition and morphology, respectively. The chemical composition of the raw material was analyzed using a PANalytic PW4030 X-ray fluorescence (XRF) spectrometer. Specifically, a MiniPAL-4 model type from Malvern Panalytical, located in Worcestershire, UK, was employed. The microstructure of the particles was examined using a scanning electron microscope (SEM using TESCAN VEGA's 4th generation Scanning Electron Microscope (SEM). All sample preparation is solid and coated with gold using the Sputter Coater NS800 model.

### 2.4. Lead Adsorption Test

The metakaolin-based AAM was crushed and then passed through a sieve with a particle size of 150 µm to be used as powder adsorbent. The larger the surface area of an adsorbent, the smaller the particle size of the adsorbent. The review also found that smaller particles can boost the efficiency of the adsorption process [14]. A study of adsorbents also supports that smaller particles can enhance adsorption efficiency. Generally, smaller particles result in a larger surface area for adsorption [30,31]. The increased surface area-to-volume ratio of smaller particles allows for greater exposure of active sites on the adsorbent,

enabling more effective adsorption of target molecules or ions [32,33]. The AAM adsorbent was washed with distilled water for about 1 h to avoid the effect of precipitation and excess amounts of sodium hydroxide on the samples and dried under vacuum at 60°C for 24 h. Then, 0.15 g of dried specimens of AAM adsorbent underwent testing under various hydrogen peroxide and surfactant doses. These tests involved using a lead nitrate solution with a fixed concentration of 300 mg/L at pH 7 and 60 minutes contact time, following the adsorption condition method outlined by Lan et al. [34] and Yan et al. [35], the metakaolin based AAM adsorbent demonstrated high lead adsorption capacity and efficient removal of lead ions.

## 3. Results and discussion

### 3.1. Raw material characterization analysis

In this study, X-ray fluorescence (XRF) analysis was employed to examine the composition of each precursor raw material used in the synthesis. The results of the XRF analysis are presented in TABLE 1, offering a detailed overview of the different metakaolin formulations utilized.

TABLE 1

Chemical composition of metakaolin

Component	wt.%
SiO <sub>2</sub>	56.7
Al <sub>2</sub> O <sub>3</sub>	34.7
TiO <sub>2</sub>	3.13
Fe <sub>2</sub> O <sub>3</sub>	2.09
P <sub>2</sub> O <sub>5</sub>	1.68
CaO	0.700
K <sub>2</sub> O	0.607
SrO	0.0530
ZrO <sub>2</sub>	0.199

The fundamental composition of metakaolin is shown in TABLE 1, demonstrating that silicon (Si) and aluminum (Al) are the two main constituents in its structure. Silica (SiO<sub>2</sub>) and alumina (Al<sub>2</sub>O<sub>3</sub>) comprise most of metakaolin's chemical composition, making up around 56.7 wt.% and 34.7 wt.%, respectively. Small quantities of impurities, such as titanium (TiO<sub>2</sub>), iron (Fe<sub>2</sub>O<sub>3</sub>), and phosphorus (P<sub>2</sub>O<sub>5</sub>), together make up around 3.13 wt.%, 2.09 wt.%, and 1.68 wt.%, respectively, are also found in addition to these primary elements. These components add up to a total weight percentage of around 98.3 wt.%. The composition analysis suggests that the metakaolin powder is a pozzolan since it has more than the acceptable threshold of 70 wt.% for pozzolans as per the ASTM C618 standard standards [36]. The ability of pozzolanic activity-rich pozzolans to improve the characteristics of cementitious materials makes them appealing. Trace amounts of strontium (SrO), zirconium (ZrO<sub>2</sub>), potassium (K<sub>2</sub>O), calcium (CaO), and various other elements were detected in the metakaolin sample. However, their concentrations were

found to be less than 1 weight percent. Although present in small quantities, these elements contribute minimally to the metakaolin material's overall composition.

Fig. 1 represents the surface morphology of metakaolin particles using Scanning Electron Microscopy (SEM) at magnifications of 5000 $\times$ .

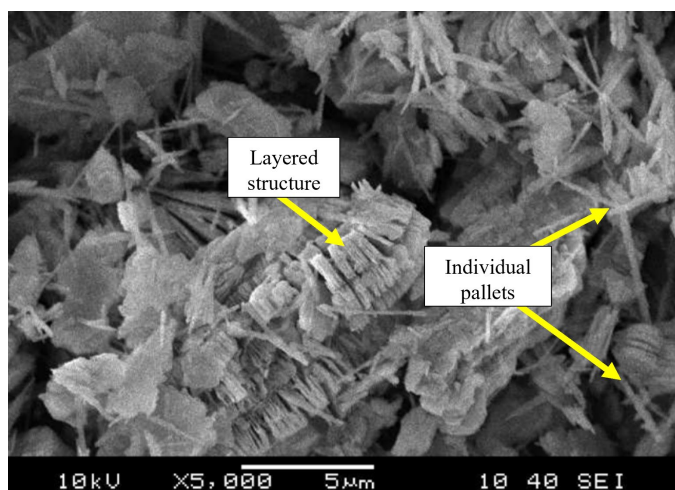


Fig. 1. Morphology of Metakaolin

According to the observations, the sample has irregularly-shaped and flake-like particles. Past researchers also supported metakaolin as a heterogeneous material of irregularly shaped particles [14,37]. Metakaolin structure is chip-like without significant porosity. Metakaolin retains the same layered structure even after thermal treatments kaolinite [38].

### 3.2. Effect on different hydrogen peroxide and surfactant content

#### 3.2.1. Porosity

The results depicted in Fig. 2 illustrate the impact of various foaming agents on the porosity of a metakaolin based AAM. Among the different amounts tested, it is observed that the addition of 1.25 wt.% foaming agent yields the highest porosity value, reaching 55.39%. Conversely, the lowest porosity is evident when no foaming agent (0 wt.%) is introduced, only at 8.99% porosity. This indicates that including a foaming agent facilitates pore formation within the alkali activated materials.

The metakaolin-based AAM porosity increases with adding foaming agent content up to 1.25 wt.%. However, it is observed that beyond 1.25 wt % foaming agent content (1.5 wt.%), the porosity begins to decline. This decline in porosity could be at higher foaming agent concentrations, and the geopolymer matrix may become saturated with the foaming agent, limiting its ability to generate additional pores. Once the saturation point is reached, further adding the foaming agent might not contribute significantly to pore formation. Moreover, excessive foaming agent content can lead to the aggregation or coalescence of

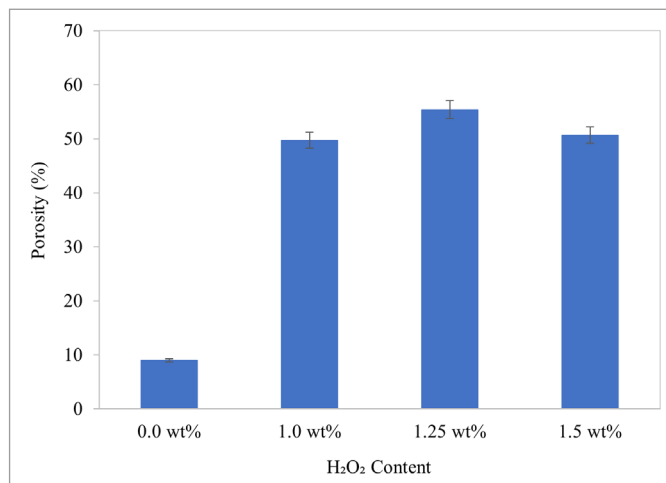


Fig. 2. The porosity of metakaolin based alkali activated materials at different hydrogen peroxide content

bubbles during the alkali activation (geopolymerization) process [39,40]. This aggregation can result in larger and fewer pores or even the collapse of existing pores, leading to decreased porosity.

Fig. 3 illustrates the impact of different surfactant (Tween 80) doses on the effectiveness of metakaolin-based AAM. According to the findings, a surfactant dosage of 3.0 wt.% demonstrated the highest porosity value (75.28%). The porosity is further enhanced with increasing surfactant content. Additionally, Ariffin et al. [41] suggest that mechanical alloying can improve the porosity of AAM adsorbents, leading to the formation of finer and more stable pores when surfactant dosage is increased. This produces a more viscous slurry paste. The sample without surfactant exhibited the lowest porosity compared to the other models since no surfactant was added, thereby lacking the contribution to pore formation. In conclusion, pores in the sample are crucial for absorbing hazardous heavy metals in water.

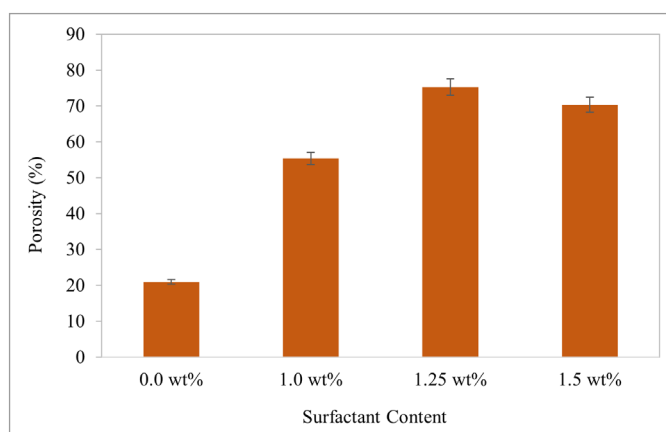


Fig. 3. The porosity of metakaolin based alkali activated materials at different surfactant content

#### 3.2.2. Water absorption and density

The densities and water absorption of metakaolin based AAM are displayed in Fig. 4. With the increase in foaming agent

content from 0% to 1.25 wt.%, the porosity of the metakaolin-based alkali-activated material (AAM) rises, reaching its peak at 55.39% water absorption. This increased porosity provides more pathways for water to penetrate the material, leading to higher water absorption. More pores allow water molecules to enter and be absorbed by capillary action [42,43]. Higher foaming agent concentrations might negatively affect the structural integrity of the geopolymer matrix. Beyond this point, the decline in water absorption can be attributed to the potential saturation of the geopolymer matrix. When the foaming agent content exceeds the optimum level (1.25%), the geopolymer may reach a saturation point where the additional foaming agent does not contribute significantly to increased porosity. Consequently, the geopolymer becomes less susceptible to absorbing water.

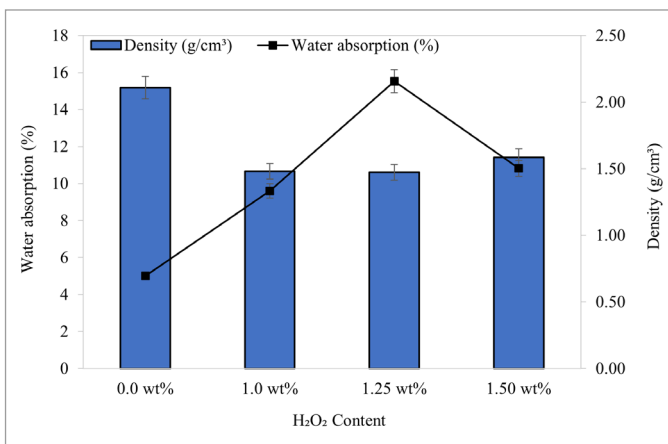


Fig. 4. Water absorption and density of metakaolin based alkali activated materials at different hydrogen peroxide content

In addition, the increase in porosity resulting from adding foaming agents up to 1.25% leads to a decrease in the overall density of the geopolymer. Introducing air or gas bubbles into the material increases its volume while maintaining a relatively constant mass, resulting in lower density. Excessive porosity can weaken the material and reduce its overall strength and durability. Beyond this threshold (1.5 wt.% H<sub>2</sub>O<sub>2</sub>), the decline in porosity and potential saturation of the geopolymer matrix can reduce the presence of air or gas bubbles. This decrease in porosity results in a denser AAM structure and, consequently, an increase in density.

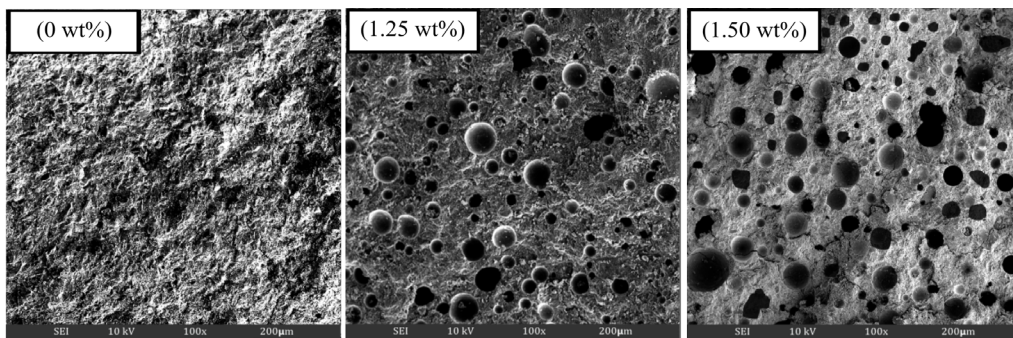


Fig. 6. Microstructural of metakaolin based AAM at different hydrogen peroxide content

On the other hand, Fig. 5 below shows the water absorption and density of metakaolin based alkali activated materials with varying percentages of surfactants. The graph demonstrates that the maximum water absorption occurs when the surfactant content reaches 3 wt.% at 22.23%. This is attributed to the sample having the highest porosity, enabling a greater water content influx. There is a significant disparity in water absorption values between 3 wt.% and 0 wt.%. The presence of surfactants, acting as stabilizing agents, influences the number of open pores on the surface, akin to their impact on the porous structure [44].

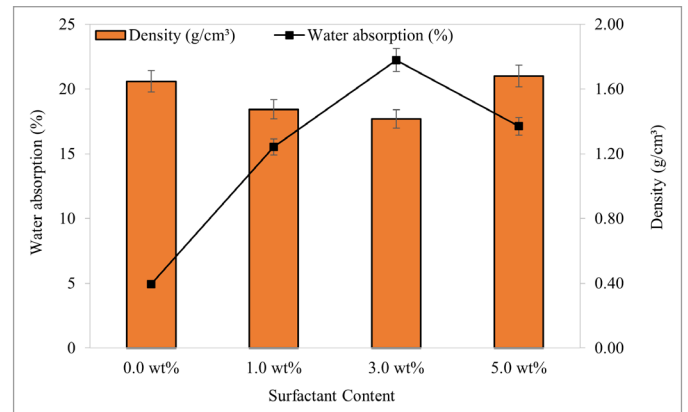


Fig. 5. Water absorption and density of metakaolin based alkali activated materials at different surfactant content

At the same time, introducing surfactants can create voids and increase the porosity of the material, reducing its density. This decrease in density is favorable for enhancing water absorption. Beyond the optimal surfactant content of 3.0 wt.% (5.0 wt.%), further increase in surfactant concentration can lead to excessive foaming and the formation of more closed cells and reduced porosity. These fast cells limit water penetration, resulting in a decline in water absorption and an increase in density.

### 3.3. Microstructural analysis

Fig. 6 presents the results of microstructural analysis using scanning electron microscopy (SEM). The control sample serves as a baseline for comparison. SEM analysis of the control sample allows for examining the natural microstructure of the

metakaolin-based AAM without any induced porosity. It provides information about the matrix's density, particle distribution, and potential voids or defects that may exist naturally within the material.

SEM analysis of AAM samples with varying hydrogen peroxide content enables a closer examination of the effects of the foaming agent on the microstructure. The analysis can reveal that SEM images can show the formation and distribution of pores within the AAM matrix. Adding hydrogen peroxide introduces gas bubbles, which act as nucleation sites for pore formation during foaming. There are any noticeable changes or variations caused by the introduction of the foaming agent at 1.25 wt.% and 1.5 wt.%. However, excessive or higher hydrogen peroxide content (1.5 wt.%) can harm the metakaolin-based alkali-activated materials (AAM) microstructure. Excessive foaming can occur during the curing process when the hydrogen peroxide content surpasses the optimal range [45,46]. This excessive foaming leads to the formation of large bubbles and the coalescence of adjacent bubbles, resulting in uneven and non-uniform pore distribution. The larger and coalesced bubbles may form fewer but larger pores, negatively impacting the microstructure. In addition, excessive foaming can adversely affect the structural integrity and mechanical strength of the AAM. The excessive presence of large bubbles that weaken the material makes it more susceptible to cracking, deformation, or failure under applied loads. This can compromise the overall performance and durability of the material.

Besides, based on Fig. 7, it can be seen that the increase of surfactant up to 3 wt.% distributed homogeneously and increased the pore diameter and pore volume of metakaolin based alkali activated materials. However, it showed a loose and porous structure unevenly dispersed throughout the matrix at 5 wt.% of Tween 80.

As the surfactant content increases, there is a noticeable decrease in smaller holes and an increase in larger pores. This effect of pore size is observed in the SEM analysis, particularly with higher surfactant concentrations. The SEM analysis reveals that surfactant content stabilizes pore size and porosity by preventing excessive pore coalescence. The figure above demonstrates slight variations in average pore diameter. When the surfactant is used with lower  $H_2O_2$  content, it produces a more uniform pore structure. However, as the  $H_2O_2$  level increases, the ability to stabilize pores decreases.

Moreover, the combination of  $H_2O_2$  and Tween 80 collaboratively creates a cell structure that is homogeneous, well-connected, and has a low relative density. Bai et al. [47] also noted that increasing the surfactant level from 1.25 to 6.25 wt.% decreases total porosity and average pore size values. The most plausible explanation for these trends is that as the surfactant amount increases, the viscosity of the slurry rises, subsequently reducing its foamability.

### 3.4. Functional group analysis

Fig. 8 depicts the IR spectra of AAM adsorbent with surfactant amounts of 1 wt.%, 3 wt.%, and 5 wt.%. Generally, the spectra exhibit distinct stretching bands and the wave numbers on the infrared spectrum range from 4,000 to 500  $cm^{-1}$ . Observing the figure, it is evident that the metakaolin-based alkali-activated materials with varying surfactant amounts display five primary absorption bands at 470.31  $cm^{-1}$ , 1014.30  $cm^{-1}$ , 1421.24  $cm^{-1}$ , 1652.99  $cm^{-1}$ , and 3458.85  $cm^{-1}$ . Additionally, hydroxyl group stretching (O-H bond) is observed at wavenumbers of 3433.09  $cm^{-1}$  and 3458.85  $cm^{-1}$ . The stretching bands at 1647.92  $cm^{-1}$  and 1652.99  $cm^{-1}$  in the metakaolin-based alkali-activated materials indicate the stretching vibration of H-OH. Furthermore, the absorption peaks at 1419.07  $cm^{-1}$  and 1421.24  $cm^{-1}$  suggest the presence of Si-O-Si and Si-O-Al in the structure, respectively.

The introduction of surfactant weakens the absorption bonds, resulting in lower transmittance and wavenumbers of the fundamental vibration, indicating decreased peak intensity. This phenomenon can be attributed to the higher surfactant content added to the mixture of alkali-activated materials.

### 3.5. Effect on foaming agent and surfactant on lead ions, Pb(II) adsorption

Fig. 9 below illustrates the absorbed amount of Pb (II) and the corresponding removal efficiency. It indicates that a higher percentage of hydrogen peroxide ( $H_2O_2$ ) in the solution enhances the adsorption of Pb (II). The maximum Pb (II) removal efficiency is observed at 1.25 wt.% of  $H_2O_2$ , where the adsorbed

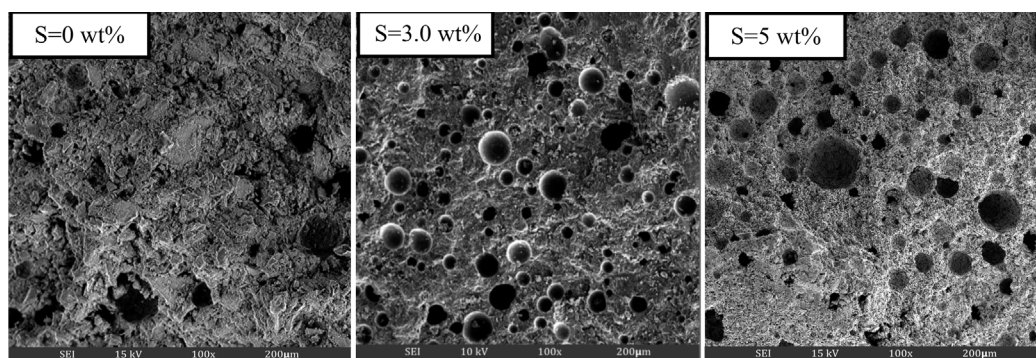


Fig. 7. Microstructural of metakaolin based AAM at different surfactant content

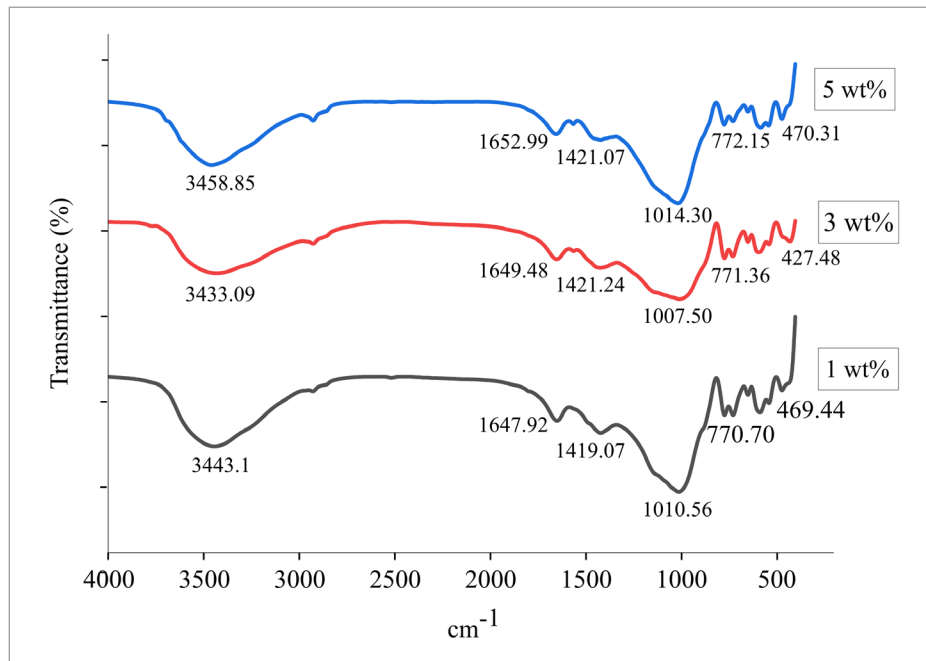


Fig. 8. FTIR spectra of metakaolin based alkali activated materials at different surfactants

amount reaches 57.17 mg/g. Conversely, the absence of  $H_2O_2$  yields the lowest removal efficiency, with only 21.13%.

However, when a foaming agent is introduced at 1.50 wt.%, the adsorption capacity and removal efficiency decrease. This decline can be attributed to excessive foaming agents unsuitable for this adsorbent.

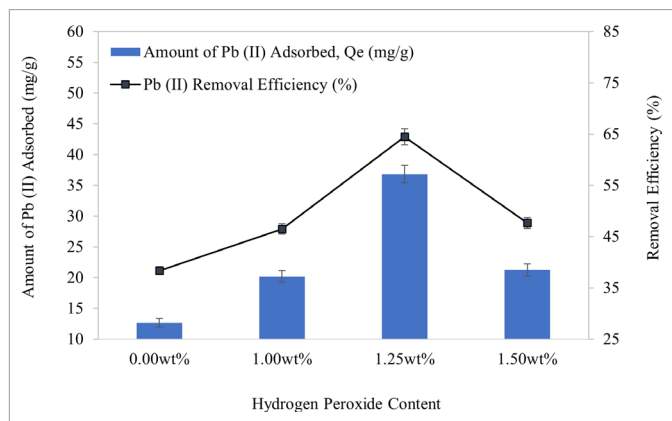


Fig. 9. Amount of Pb(II) adsorbed and removal efficiency on different hydrogen peroxide content

The foaming agent is critical in the solution and possesses adsorption ability. Its addition results in the loosening of the surfaces of the AAM adsorbent, leading to the creation of more pore structures. This alteration proves beneficial in reducing the diffusion resistance of ions within the adsorbent, ultimately increasing the adsorption rate and capacity. The pore structure and surface area are vital for adsorbents as they facilitate enhanced interactions between the adsorbate and the active adsorption sites. In conclusion, incorporating a foaming agent increases porosity, improving adsorption.

Furthermore, Fig. 10 illustrates the outcomes of Pb(II) adsorption and the related removal efficacy at various surfactant concentrations. Based on the graphical representation, it can be observed that the incorporation of a surfactant at a concentration of 3.00 wt.% in the AAM adsorbent yielded the highest adsorption capacity for Pb(II) at 86.27 mg/g, along with a removal efficiency of 64.70%. This outcome surpassed the performance exhibited by other concentrations of the surfactant. Using a surfactant at a concentration of 5.00 wt.% led to a decline in removal efficiency, measuring 46.23%. Without adding a surfactant, the AAM adsorbent showed the lowest removal efficiency and amount of Pb(II) adsorbed.

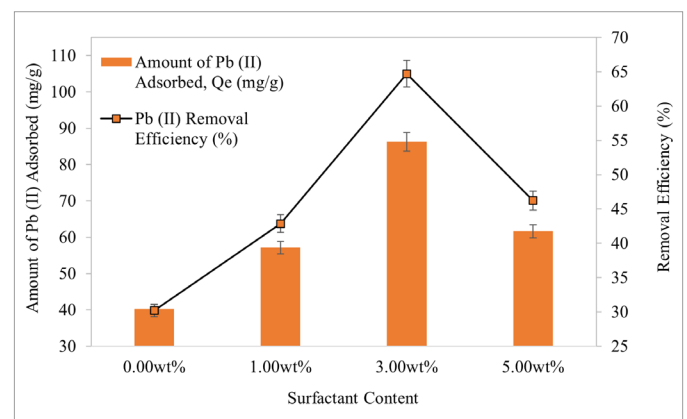


Fig. 10. Amount of Pb(II) adsorbed and removal efficiency on different surfactant content

When a combination of surfactants and a foaming agent is utilized, it forms porous characteristics in the AAM adsorbent. The properties of the surfactants play a crucial role in creating porous geopolymers through direct foaming. The addition of

surfactant rapidly increases the slurry's viscosity. The surfactant aids in generating finer and more stable pores, and as the amount of surfactant increases, it leads to a more viscous slurry paste.

The observed pattern indicates that the adsorption capacity decreases when the surfactant amount reaches 5 wt.%. The addition of surfactant can increase the specific surface area [48,49]. This finding is supported by evidence from Bai et al. [43], which states that increasing the surfactant content from 3 wt.% to 6.25 wt.% results in decreased total porosity and average pore size values. The most likely interpretation of these trends is that as the amount of surfactant increases, the viscosity of the slurry rises while the foamability decreases [50].

#### 4. Conclusions

In summary, the introduction of foaming agents and surfactants has proven to significantly enhance the adsorption capacity of alkali-activated materials (AAM) for lead ions. The optimal concentrations of 1.25 wt.% foaming agent and 3 wt.% surfactant have yielded remarkable results, with highest porosity value (75.28%) achieving the highest recorded adsorption capacity (86.27 mg/g) and removal efficiency (64.70%) for lead ions in 1 hour contact time. The foaming agent played a crucial role in creating a porous structure, amplifying pore diameter and volume, has boosted adsorption rate and capacity while the contribution of surfactant in preserving pore stability and overall porosity of the AAM adsorbent has been pivotal. The research study concludes the effects of foaming agents and surfactants on alkali-activated materials can lead to the development of improved adsorbents for various pollutants beyond lead ions. The study successfully determined the ideal parameters for achieving the highest possible efficiency in removing lead ions. These parameters incorporate a concentration of 1.25 wt.% of H<sub>2</sub>O<sub>2</sub> and 3 wt.% of Tween 80 hold significant promise for the advancement of effective adsorbents, particularly in the realm of wastewater treatment processes, and contribute to the ongoing pursuit of environmental remediation solutions.

#### Acknowledgments

The author would like to acknowledge the Fundamental Research Grant Scheme (FRGS) support under a grant number of FRGS/1/2019/TK10/UNIMAP/02/21 from the Ministry of Higher Education Malaysia.

#### REFERENCES

- [1] M.R. Awual, M.M. Hasan, M.A. Khaleque, M.C. Sheikh, Treatment of copper(II) containing wastewater by a newly developed ligand based facial conjugate materials. *Chemical Engineering Journal* **288**, 368-376, Mar. (2016). DOI: <https://doi.org/10.1016/j.cej.2015.11.108>
- [2] I. Luhar, S. Luhar, M.M.A.B Abdullah, R. Razak, P. Vizureanu, A.V. Sandu, A. Matasaru, A state-of-the-art review on innovative geopolymer composites designed for water and wastewater treatment. *Materials* **14**, 23, MDPI, (2021). DOI: <https://doi.org/10.3390/ma14237456>
- [3] D.G. Della Rocca, R.M. Peralta, R.A. Peralta, E. Rodríguez-Castellón, R. de Fatima Peralta Muniz Moreira, Adding value to aluminosilicate solid wastes to produce adsorbents, catalysts and filtration membranes for water and wastewater treatment. *J. Mater. Sci.* **56**, 2, 1039-1063 (2021). DOI: <https://doi.org/10.1007/s10853-020-05276-0>
- [4] S.F. Ahmed, M. Mofjijur, S. Nuzhat, A. Tasnim, N. Rafa, A. Uddin, A. Inayat, T.M.I. Mahlia, H. Chyuan, W. Yi, L. Show, Recent developments in physical, biological, chemical, and hybrid treatment techniques for removing emerging contaminants from wastewater. *J. Hazard. Mater.* **416**, 125912 (2021). DOI: <https://doi.org/10.1016/j.jhazmat.2021.125912>
- [5] I. Kara, D. Tunc, F. Sayin, S.T. Akar, Study on the performance of metakaolin based geopolymer for Mn(II) and Co(II) removal. *Appl. Clay. Sci.* **161**, 184-193 (2018). DOI: <https://doi.org/10.1016/j.clay.2018.04.027>
- [6] J. Zhang, B. Liu, S. Zhang, A review of glass ceramic foams prepared from solid wastes: Processing, heavy-metal solidification and volatilization, applications. *Science of the Total Environment*, **781**, Elsevier B.V., 10 (2021). DOI: <https://doi.org/10.1016/j.scitotenv.2021.146727>
- [7] Y. Liu, C. Yan, Z. Zhang, H. Wang, S. Zhou, W. Zhou, A comparative study on fly ash, geopolymer and faujasite block for Pb removal from aqueous solution. *Fuel* **185**, 181-189 (2016). DOI: <https://doi.org/10.1016/j.fuel.2016.07.11>
- [8] X. Feng, S. Yan, S. Jiang, K. Huang, X. Ren, X. Du, P. Xing, Green Synthesis of the Metakaolin/slag Based Geopolymer for the Effective Removal of Methylene Blue and Pb (II). *Silicon* **14**, 6965-6979 (2022). DOI: <https://doi.org/10.1007/s12633-021-01439-z>
- [9] Y. Zhu, Z. Zheng, Y. Deng, C. Shi, Z. Zhang, Advances in immobilization of radionuclide wastes by alkali activated cement and related materials. *Cem. Concr. Compos.* **126** (2022). DOI: <https://doi.org/10.1016/j.cemconcomp.2021.104377>
- [10] Y. Wu, B. Lu, T. Bai, H. Wang, F. Du, Y. Zhang, L. Cai, C. Jiang, W. Wang, Geopolymer, green alkali activated cementitious material: Synthesis, applications and challenges. *Construction and Building Materials* **224**, Elsevier Ltd, 930-949 (2019). DOI: <https://doi.org/10.1016/j.conbuildmat.2019.07.112>
- [11] T. Luukkonen, Z. Abdollahnejad, J. Yliniemi, P. Kinnunen, M. Illikainen, One-part alkali-activated materials: A review. *Cem Concr Res* **103**, 2017, 21-34 (2018). DOI: <https://doi.org/10.1016/j.cemconres.2017.10.001>
- [12] P.K. Pachana, U. Rattanasak, P. Jitsangiam, P. Chindaprasirt, Alkali-activated material synthesized from palm oil fuel ash for Cu/Zn ion removal from aqueous solutions. *Journal of Materials Research and Technology* **13**, 440-448 (2021). DOI: <https://doi.org/10.1016/j.jmrt.2021.04.065>
- [13] T. Luukkonen, A. Heponiemi, H. Runtti, J. Pesonen, J. Yliniemi, U. Lassi, Application of alkali-activated materials for water and

- wastewater treatment: a review. *Rev. Environ. Sci. Biotechnol.* **18**, 2, 271-297 (2019).  
DOI: <https://doi.org/10.1007/s11157-019-09494-0>
- [14] M. Ibrahim, W.M.W. Ibrahim, M.M.A.B Abdullah, M. Nabialek, R. Putra Jaya, M. Setkit, R. Ahmad, B. Jež, Synthesis of Metakaolin Based Alkali Activated Materials as an Adsorbent at Different Na<sub>2</sub>SiO<sub>3</sub>/NaOH Ratios and Exposing Temperatures for Cu<sup>2+</sup> Removal. *Materials* **16**, 3 (2023).  
DOI: <https://doi.org/10.3390/ma16031221>
- [15] T. Lan, P. Li, X. Li, J. Guo, Q. Huang, J.J. Geng, Q. Zhao, W. Yang, S. Guo, Influence of modulus of alkaline activator on the removal of Pb<sup>2+</sup> by mesoporous geopolymer adsorbent. *Environmental Technology (United Kingdom)* **43** (27), 4269-4278 (2022).  
DOI: <https://doi.org/10.1080/09593330.2021.1946597>
- [16] P. Perez-Cortes, J.I. Escalante-Garcia, Gel composition and molecular structure of alkali-activated metakaolin-limestone cements. *Cem. Concr. Res.* **37**, no. September, p. 106211 (2020).  
DOI: <https://doi.org/10.1016/j.cemconres.2020.106211>
- [17] J. Carvalheiras, R.M. Novais, J.A. Labrincha, Metakaolin/red mud-derived geopolymer monoliths: Novel bulk-type sorbents for lead removal from wastewaters. *Appl. Clay. Sci.* **232** (2023).  
DOI: <https://doi.org/10.1016/j.clay.2022.106770>
- [18] M. Ibrahim, W. Mastura Wan Ibrahim, M. Mustafa Al Bakri Abdullah, A. Syaqui Sauffi, A Review of Geopolymer Based Metakaolin Membrane as an Effective Adsorbent for Waste Water Treatment. *IOP Conf. Ser. Mater. Sci. Eng.* **864**, 1 (2020).  
DOI: <https://doi.org/10.1088/1757-899X/864/1/012128>
- [19] J. Karuppaiyan, A. Mullaimalar, R. Jeyalakshmi, Adsorption of dyestuff by nano copper oxide coated alkali metakaoline geopolymer in monolith and powder forms: Kinetics, isotherms and microstructural analysis. *Environ. Res.* **218** (2023).  
DOI: <https://doi.org/10.1016/j.envres.2022.115002>
- [20] T.R. Barbosa, E.L. Foletto, G.L. Dotto, S.L. Jahn, Preparation of mesoporous geopolymer using metakaolin and rice husk ash as synthesis precursors and its use as potential adsorbent to remove organic dye from aqueous solutions. *Ceram. Int.* **44**, 1, 416-423 (2018). DOI: <https://doi.org/10.1016/j.ceramint.2017.09.193>
- [21] H. Jin, Y. Zhang, Q. Wang, Q. Chang, C. Li, Rapid removal of methylene blue and nickel ions and adsorption/desorption mechanism based on geopolymer adsorbent. *Colloids and Interface Science Communications* **45** (2021).  
DOI: <https://doi.org/10.1016/j.colcom.2021.100551>
- [22] C. Xu, W. Yu, K. Zheng, C. Ling, S. Yu, L. Jiang, Novel composite oxygen-containing resins with effective adsorption towards anilines: physical & chemical adsorption. *Journal of Chemical Technology and Biotechnology* **95**, 8, 2187-2194 (2020).  
DOI: <https://doi.org/10.1002/jctb.6405>
- [23] S.A. Rasaki, Z. Bingxue, R. Guarecuco, T. Thomas, Y. Minghui, Geopolymer for use in heavy metals adsorption, and advanced oxidative processes: A critical review. *J. Clean. Prod.* **213**, 42-58 (2019). DOI: <https://doi.org/10.1016/j.jclepro.2018.12.145>
- [24] H. Wu, S. Lin, X. Cheng, J. Chen, Y. Ji, D. Xu, M. Kang, Comparative study of strontium adsorption on muscovite, biotite and phlogopite. *J. Environ. Radioact.* **225**, no. September 106446 (2020). DOI: <https://doi.org/10.1016/j.jenvrad.2020.106446>
- [25] L. Panda, S.K. Jena, S.S. Rath, P.K. Misra, Heavy metal removal from water by adsorption using a low-cost geopolymer. *Environmental Science and Pollution Research* **27**, 19, 24284-2429 (2020).  
DOI: <https://doi.org/10.1007/s11356-020-08482-0>
- [26] N.A. Jaya, Y.M. Liew, C.Y. Heah, M.M.A.B. Abdullah, Effect of solid-to-liquid ratios on metakaolin geopolymers Effect of Solid-to-liquid Ratios on Metakaolin Geopolymer. *AIP Conference Proceedings* **2045**, 1, AIP Publishing (2018).  
DOI: <https://doi.org/10.1063/1.5080912>
- [27] ASTM C642, Standard Test Method for Density, Absorption and Voids in Hardened Concrete.
- [28] ASTM D792, Standard Test Methods for Density and Specific Gravity (Relative Density) of Plastics by Displacement.
- [29] ASTM D570, Standard Test Method for Water Absorption of Plastics.
- [30] Y. Dong, M. Gao, Z. Song, W. Qiu, As(III) adsorption onto different-sized polystyrene microplastic particles and its mechanism. *Chemosphere* **239**, Jan. (2020).  
DOI: <https://doi.org/10.1016/j.chemosphere.2019.124792>
- [31] F. Wang, W. Yang, P. Cheng, S. Zhang, S., W. Jiao, Y. Sun, Adsorption characteristics of cadmium onto microplastics from aqueous solutions. *Chemosphere* **235**, 1073-1080, Nov. (2019).  
DOI: <https://doi.org/10.1016/j.chemosphere.2019.06.196>
- [32] S. Rajendran, A.K. Priya, P. Senthil Kumar, T.K.A. Hoang, K. Sekar, K.Y. Chong, K.S. Khoo, H. S. Ng, P.L. Show, A critical and recent developments on adsorption technique for removal of heavy metals from wastewater-A review. *Chemosphere* **303**, Sep. (2022).  
DOI: <https://doi.org/10.1016/j.chemosphere.2022.135146>
- [33] G.T. Tee, X.Y. Gok, W.F. Yong, Adsorption of pollutants in wastewater via biosorbents, nanoparticles and magnetic biosorbents: A review. *Environmental Research* **212**, Academic Press Inc., Sep. 01, (2022).  
DOI: <https://doi.org/10.1016/j.envres.2022.113248>
- [34] T. Lan S. Guo, X. Li, J. Guo, T. Bai, Q. Zhao, W. Yang, P. Li, Mixed precursor geopolymer synthesis for removal of Pb(II) and Cd(II). *Mater. Lett.* **274**, (2020).  
DOI: <https://doi.org/10.1016/j.matlet.2020.127977>
- [35] C. Yan, L. Guo, D. Ren, P. Duan, Novel composites based on geopolymer for removal of Pb(II). *Mater. Lett.* **239**, 192-195 (2019). DOI: <https://doi.org/10.1016/j.matlet.2018.12.105>
- [36] ASTM C618 – 12 Standard Specification for Coal Fly Ash and Raw or Calcined Natural Pozzolan for Use in Concrete.
- [37] M. Ibrahim, W.M. Wan Ibrahim, M.M.A.B. Abdullah, A.S. Sauffi, P. Vizureanu, Effect of Solids-To-Liquids and Na<sub>2</sub>SiO<sub>3</sub>-To-NaOH on Metakaolin Membrane Geopolymers (1). *Arch. Metall. Mater.* **67**, 695–702 (2022).  
DOI: <https://doi.org/10.24425/amm.2022.137808>
- [38] N.A. Jaya, L. Yun-Ming, M. Mustafa, A. Bakri, Thermophysical Properties of Metakaolin Geopolymers Based on Na<sub>2</sub>SiO<sub>3</sub> / NaOH Ratio. *Solid State Phenomena* **280**, 487-493 (2018).  
DOI: <https://doi.org/10.4028/www.scientific.net/SSP.280.487>
- [39] J. Shi, B. Liu, Y. Liu, E. Wang, Z. He, H. Xu, X. Ren, Preparation and characterization of lightweight aggregate foamed geopolymer

- concretes aerated using hydrogen peroxide. *Constr. Build. Mater.* **256** (2020).  
DOI: <https://doi.org/10.1016/j.conbuildmat.2020.119442>
- [40] M. Nodehi, A comparative review on foam-based versus light-weight aggregate-based alkali-activated materials and geopolymer. *Innovative Infrastructure Solutions*, **6**, no. 4. Springer Science and Business Media Deutschland GmbH, (2021).  
DOI: <https://doi.org/10.1007/s41062-021-00595-w>
- [41] N. Ariffin, M.M.A.B. Abdullah, P. Postawa, S.Z.A. Rahim, M.R.R.M.A. Zainol, R.P. Jaya, A. Śliwa, M.F. Omar, J.J. Wysocki, K. Błoch, M. Nabiałek, Effect of aluminium powder on kaolin-based geopolymer characteristic and removal of Cu<sup>2+</sup>. *Materials* **14**, 4, 1-19 (2021). DOI: <https://doi.org/10.3390/ma14040814>
- [42] C. Bai, P. Colombo, Processing, properties and applications of highly porous geopolymers: A review. *Ceram. Int.* **44**, 14, 16103-16118 (2018).  
DOI: <https://doi.org/10.1016/j.ceramint.2018.05.219>
- [43] C. Bai, T. Ni, Q. Wang, H. Li, P. Colombo, Porosity, mechanical and insulating properties of geopolymer foams using vegetable oil as the stabilizing agent. *J. Eur. Ceram. Soc.* **38**, 2, 799-805 (2018). DOI: <https://doi.org/10.1016/j.jeurceramsoc.2017.09.021>
- [44] Y. Qiao et al., Effects of surfactants / stabilizing agents on the microstructure and properties of porous geopolymers by direct foaming. *Journal of Asian Ceramic Societies* **9**, 1, 412-423 (2021). DOI: <https://doi.org/10.1080/21870764.2021.1873482>
- [45] W.M.W. Ibrahim, K. Hussin, M.M.A.B. Abdullah, A.A. Kadir, Geopolymer lightweight bricks manufactured from fly ash and foaming agent. *AIP Conf. Proc.* 1835 (2017).  
DOI: <https://doi.org/10.1063/1.4981870>
- [46] A. Tarameshloo, E.N. Kani, A. Allahverdi, E.N. Kani, G. Engineering, Performance evaluation of foaming agents in cellular concrete based on foamed alkali-activated slag. *Canadian Journal of Civil Engineering* **44** (11), 1-30 (2017).  
DOI: <https://doi.org/10.1139/cjce-2016-0491>
- [47] C. Bai, G. Franchin, H. Elsayed, A. Zaggia, L. Conte, H. Li, P. Colombo, High-porosity geopolymer foams with tailored porosity for thermal insulation and wastewater treatment. *J. Mater. Res.* **32**, 17, 3251-3259 (2017).  
DOI: <https://doi.org/10.1557/jmr.2017.127>
- [48] H. Kong, S.C. Cheu, N.S. Othman, S.T. Song, N. Saman, K. Johari, H. Mat, Surfactant modification of banana trunk as low-cost adsorbents and their high benzene adsorptive removal performance from aqueous solution. *RSC Adv.* **6**, 29, 24738-24751 (2016). DOI: <https://doi.org/10.1039/c6ra00911e>
- [49] S. Tamjidi, B.K. Moghadas, H. Esmacili, F. Shakerian Khoo, G. Gholami, M. Ghasemi, Improving the surface properties of adsorbents by surfactants and their role in the removal of toxic metals from wastewater: A review study. *Process Safety and Environmental Protection* **148**, Institution of Chemical Engineers, 775-795 (2021).  
DOI: <https://doi.org/10.1016/j.psep.2021.02.003>
- [50] P. Amani, R. Miller, A. Javadi, M. Firouzi, Pickering foams and parameters influencing their characteristics. *Advances in Colloid and Interface Science* **301**, Elsevier B.V. (2022). DOI: <https://doi.org/10.1016/j.cis.2022.102606>